PERGAMON

International Journal of Heat and Mass Transfer 43 (2000) 2273–2287

International Journal of HEAT and MASS TRANSFER

www.elsevier.com/locate/ijhmt

Analysis of forced convection in pipes and channels with the simplified Phan-Thien–Tanner fluid

F.T. Pinho [a], P.J. Oliveira [b,*]

[a] Centro de Estudos de Fenómenos de Transporte, Departamento de Engenharia Mecânica, Faculdade de Engenharia, Universidade do Porto, Rua dos Bragas, 4050-123 Porto, Portugal

[b] Departamento de Engenharia Electromecânica, Universidade da Beira Interior Rua Marquês D'Ávila e Bolama, 6200 Covilha, Portugal

Received 24 March 1999; received in revised form 1 October 1999

Abstract

Analytical solutions are derived for the temperature distribution and heat transfer coefficient in forced convection of a viscoelastic fluid obeying the simplified Phan-Thien–Tanner constitutive equation in laminar pipe and plane channel flows. The results are valid for fully developed thermal and hydrodynamic flow conditions with a constant heat flux imposed at the wall and include the investigation of the effects of viscous dissipation. A nonvanishing value of the extensional parameter of the fluid model is shown to be essential for the solution to differ significantly from that for a Newtonian, or an elastic fluid without extensibility. Elasticity, only when combined with extensibility, is shown to increase the heat transfer and to reduce the range of temperatures present inside a duct. These beneficial effects of fluid elasticity are enhanced by viscous dissipation.

1. Introduction

The Phan-Thien–Tanner (PTT) constitutive equation was derived from considerations of network theory by Phan-Thien and Tanner [1] and is a simple, yet adequate model, often used to simulate the rheological behaviour of polymer melts and concentrated solutions as in Quinzani et al. [2], Laun and Schuch [3] and Wu et al. [4]. In its general form it is written as

$$Y(\mathrm{tr}\,\tau, T)\tau + \lambda\left(\overset{\triangledown}{\tau} + \xi \mathbf{D}\cdot\tau + \xi\tau\cdot\mathbf{D}^{\mathrm{T}}\right) = 2\eta\mathbf{D} \tag{1}$$

where $\overset{\triangledown}{\tau}$ stands for Oldroyd's upper convected derivative of the stress tensor τ

$$\overset{\triangledown}{\tau} = \frac{\mathrm{D}\mathbf{u}}{\mathrm{D}t} - \tau\cdot\nabla\mathbf{u} - \nabla\mathbf{u}^{\mathrm{T}}\cdot\tau \tag{2}$$

In Eq. (1), λ is the relaxation time, ξ is an adjustable parameter related to the slip velocity between the molecular network and the continuum medium, η is the viscosity coefficient equal to the product of the relaxation time by the relaxation modulus λG, and $\mathbf{D}$ is the rate of strain tensor. The stress-coefficient function Y is related to the rate of destruction of junctions in the molecular network and can be decoupled as

$$Y(\mathrm{tr}\,\tau, T) = \phi(T) f(\mathrm{tr}\,\tau) \tag{3}$$

where T is the temperature and tr τ is the trace of the stress tensor τ. A simplified version of the full PTT

* Corresponding author. Fax: +351-275-320820.

E-mail addresses: fpinho@fe.up.pt (F.T. Pinho), pjpo@ubi.pt (P.J. Oliveira).

0017-9310/00/$ - see front matter
PII: S0017-9310(99)00303-8

Nomenclature

a	non-dimensional parameter defined in Eq. (16b)
Br	Brinkman number as defined in Eq. (26)
c_p	specific heat
$\mathbf{D}$	rate of strain tensor
De	Deborah number
D_H	hydraulic diameter
h	heat transfer coefficient
H	half-width of channel
k	thermal conductivity
Nu	Nusselt number
p	pressure
$\dot{q}_w$	heat flux at the wall
r	radial coordinate
R	pipe radius
T	temperature
$\bar{T}$	cross-sectional average temperature
T_c	centreline temperature
T_w	wall temperature
$\mathbf{u}$	velocity vector
$\bar{u}$	cross-sectional average velocity
$\bar{u}_N$	cross-sectional average velocity for a Newtonian fluid
x	longitudinal coordinate
y	transverse coordinate in channel flow
Y	stress coefficient function
α	thermal diffusivity
ε	parameter of PTT model
Φ	viscous dissipation function
$\dot{\gamma}$	shear rate
η	viscosity coefficient of PTT model
λ	relaxation time of PTT model
θ	non-dimensional temperature defined in Eq. (31)
ρ	density
τ	stress tensor
ξ	parameter of PTT model

considers affine motions only and in this case $\xi = 0$. The fluid still exhibits shear-thinning because of the term involving ε, but to a lower extent. This simplified version of the PTT constitutive equation (SPTT) becomes

$$Y(\mathrm{tr}\,\tau, T)\tau + \lambda \overset{\nabla}{\tau} = 2\eta\mathbf{D} \tag{4}$$

Following Phan-Thien [5] the function $\phi(T)$ is arbitrarily set to unity at the reference temperature at which the relaxation spectrum is measured and the material parameters are determined.

The stress-dependent part of the stress-coefficient function has an exponential form

$$f(\mathrm{tr}\,\tau) = \exp\left(\frac{\varepsilon\lambda}{\eta}\mathrm{tr}\,\tau\right) \tag{5}$$

which may be linearised when the factor in brackets is small, as:

$$f(\mathrm{tr}\,\tau) = 1 + \frac{\varepsilon\lambda}{\eta}\mathrm{tr}\,\tau \tag{6}$$

Although the exponential form of the stress-coefficient is more adequate for the prediction of polymer melts (Larson [6]), significant differences between the two formulations require a considerable amount of molecular deformation, particular the extensional deformation. From the physical point of view, the linearisation is accurate when the molecular deformation is rather limited as in weak flows (Tanner's classification [7]). The pipe and channel flows analysed here are weak flows, according to that classification; for these flows the deformation of the molecules is small and so the linear equation (6) is not too far from its exponential form in Eq. (5). These are shear-dominated flows for which most nonlinear models, such as the PTT model, provide accurate descriptions of shear properties of polymer melts, as demonstrated by Peters et al. [8]. The exception here is the failure of PTT to predict a non-zero second normal stress difference, but this quantity is totally irrelevant to the hydrodynamics of fully developed pipe and channel flows. In complex strong flows the accuracy of PTT is not so good, but its use is favoured by the ability to control separately, and to some extent, its shear and elongational properties.

In the above equations ε is the second free parameter and is related to the elongational behaviour of the model. It imposes an upper limit to the elongational viscosity and that limit is proportional to the inverse of ε. Note that $\varepsilon = 0$ is equivalent to the upper-convected Maxwell model which has an unbounded elongational viscosity in simple extensional flow. As will be shown, a finite value of the extensional capability of the fluid ($\varepsilon \neq 0$) makes its heat transfer characteristics considerably different from the case of $\varepsilon = 0$. In addition, ε may have an influence on the shear properties, imparting shear-thinning to the fluid provided the parameter is not too small (Phan-Thien [5] has shown no effect of ε when it is of the order of 10^{-2}).

Viscoelastic fluid flow through pipes and channels is clearly relevant from an industrial point of view. In polymer processing, melts flow in pipes before extrusion, usually at high temperatures, hence knowledge of the temperature distribution and heat transfer coefficients is also of great importance. The quality of the final product depends on the ability to avoid appearance of hot spots or instabilities during the manufacturing process. These hot spots tend to occur because the low thermal conductivity of polymers induces considerable nonuniform temperature variations that are accentuated by viscous heating and property variations with temperature. Knowledge of the temperature distribution in forced convection appears therefore, as an essential requirement to the good design of polymer processing equipment. This is the scope of the current work.

The analytical hydrodynamic solution of the simplified PTT fluid flowing in a pipe has been obtained recently by Oliveira and Pinho [9]. Based on that solution we analyse now the corresponding heat transfer problem and derive the temperature distribution and heat transfer coefficient for pipe and channel flows of the simplified form of the PTT model with a linear stress-coefficient. Note that for inelastic non-Newtonian fluids there is already a wealth of information, in particular for fluids obeying the power law model (see, for instance, Irvine and Karni [10]).

In the next section, the problem is formulated and the solution of the corresponding hydrodynamic problem will be presented. Then, the analytical heat transfer solution will be derived in detail and the effects of fluid elasticity and viscous dissipation on the relevant quantities will be discussed. The derivation and discussion of results will be carried out in detail for the pipe flow geometry only, whereas for the equivalent planar geometry the final results will be presented without further comment.

2. Formulation of the problem

The flow is considered to be fully developed both thermally and hydrodynamically. It is also assumed that the flow is steady, laminar and has constant properties, i.e., no dependence of the fluid properties and model parameters on temperature will be considered. A constant wall heat transfer flux constitutes the investigated boundary condition.

Fluids found in polymer processing (polymer melts and concentrated solutions) are usually very viscous and industrial flows frequently involve large velocity gradients, thus viscous dissipation effects can be important and therefore will be taken into account. However, as mentioned above, we will consider in this analysis that the temperature variations will not be high enough to impose significant changes in fluid properties.

Thermal and thermodynamic properties of polymer solids are anisotropic as they are intimately related to their molecular structure. As the polymer melts its chains tend towards random configurations, thus these properties become isotropic after some characteristic time of the fluid. Otherwise, the need to consider a second order thermal conductivity tensor to account for nonisotropic heat conduction would arise. These properties also vary with temperature and pressure, but experimental data and previous heat transfer work relevant to polymer melts (Tadmor and Gogos [11], Bird et al. [12]) indicate that the assumption of constant thermal conductivity and heat capacity does not seriously affect the results, whereas the assumption of constant density restricts the analysis to forced convection. In any case, the properties to be used in calculations with the formulas derived in this work should be evaluated at the average temperature of the fluids in order to improve accuracy.

It is also assumed that Fourier's law of heat conduction is valid and that the internal energy and thermal conductivity do not depend explicitly on the velocity gradient or other kinematic quantities. These are standard, reasonable assumptions in heat transfer calculations of non-Newtonian fluids as discussed in Section 4.4 of Bird et al. [12], Section 9.1 of Tanner [7] and in Tadmor and Gogos [11]. The equation to be solved in the axisymmetric case is the energy transport equation with provision for viscous dissipation

$$k\frac{1}{r}\frac{\partial}{\partial r}\left(r\frac{\partial T}{\partial r}\right)+\Phi=\rho c_p u\frac{\partial T}{\partial x} \tag{7}$$

where k,ρ and c_{p} stand for the thermal conductivity, density and specific heat, respectively. The temperature T varies radially r and axially x, u stands for the longitudinal velocity component and Φ is the dissipation function which is generaly defined as

$$\Phi\equiv\tau_{ij}\frac{\partial u_i}{\partial x_j} \tag{8}$$

The thermal boundary conditions are axisymmetry

$$\left.\frac{\partial T}{\partial r}\right|_{r=0}=0 \tag{9}$$

and a constant wall heat flux,

$$-k\left.\frac{\partial T}{\partial r}\right|_{r=R}=\dot{q}_w \tag{10}$$

which is negative when it enters the pipe.

For the flow conditions under scrutiny the dissipation function involves the shear component exclusively, i.e.,

$$\Phi = \tau_{xr}\dot{\gamma}_{xr} = \tau_{xr}\frac{\partial u}{\partial r} \tag{11}$$

with the velocity and shear stress profiles taking the forms derived by Oliveira and Pinho [9] and given in Eqs. (12) and (13), respectively.

$$\frac{u}{\bar{u}} = 2\frac{\overline{u_N}}{\bar{u}}\left[1-\left(\frac{r}{R}\right)^2\right]\left\{1+16\varepsilon De^2\left(\frac{\overline{u_N}}{\bar{u}}\right)^2\left[1+\left(\frac{r}{R}\right)^2\right]\right\} \tag{12}$$

$$\frac{\tau_{xr}}{4\eta\bar{u}/R} = -\frac{\overline{u_N}}{\bar{u}}\left(\frac{r}{R}\right) \tag{13}$$

The shear rate $\dot{\gamma}_{xr}$ is given by

$$\frac{\dot{\gamma}_{xr}}{4\bar{u}/R} = -\frac{\overline{u_N}}{\bar{u}}\left(\frac{r}{R}\right)\left\{1+32\varepsilon De^2\left(\frac{\overline{u_N}}{\bar{u}}\right)^2\left(\frac{r}{R}\right)^2\right\} \tag{14}$$

In Eqs. (12) and (14) the nondimensional group $De = \lambda\bar{u}/R$ is the Deborah number, a measure of the level of elasticity in the fluid. It is based on the cross-sectional average velocity $\bar{u}$ for the PTT fluid. $\overline{u_N}$ is the average velocity for a Newtonian fluid flowing under the same pressure gradient $\mathrm{d}p/\mathrm{d}x$

$$\overline{u_N} \equiv \frac{-(\mathrm{d}p/\mathrm{d}x)R^2}{8\eta} \tag{15}$$

and was shown to be given by:

$$\frac{\overline{u_N}}{\bar{u}} = \frac{432^{1/6}\left(\delta^{2/3}-2^{2/3}\right)}{6b^{1/2}\delta^{1/3}} \text{ with}$$

$$\delta = \left(3^3 b+4\right)^{1/2} + 3^{3/2}b^{1/2} \text{ and}$$

$$b = \frac{64}{3}\varepsilon De^2 \tag{16a}$$

For the following derivations it will be advantageous to use a modification of b, which we will designate as a, and is defined below.

$$a \equiv 16\varepsilon De^2\left(\frac{\overline{u_N}}{\bar{u}}\right)^2 \tag{16b}$$

This nondimensional parameter gives a measure of both the extensional and the elastic properties of the fluid.

3. Analytical solution

3.1. Pipe flow

The constant wall flux boundary condition (Eq. (10)) implies that the cross-section average temperature ($\bar{T}$) must increase longitudinally at a constant rate. This, together with the condition of thermal fully developed flow, implies a constant longitudinal gradient of temperature $\partial T/\partial x$.

Eqs. (11)–(14) are back-substituted into the energy equation, which can then be integrated for the first time. The axisymmetry boundary condition (9) is applied next to solve the first constant of integration leading to the radial distribution of the gradient of temperature

$$\frac{\partial T}{\partial r} = \frac{2R\overline{u_N}}{\alpha}\frac{\mathrm{d}T}{\mathrm{d}x}\left[\frac{(1+a)}{2}\frac{r}{R}-\frac{1}{4}\left(\frac{r}{R}\right)^3-\frac{a}{6}\left(\frac{r}{R}\right)^5\right] - \frac{16\eta\overline{u_N}^2}{kR}\left[\frac{1}{4}\left(\frac{r}{R}\right)^3+\frac{a}{3}\left(\frac{r}{R}\right)^5\right] \tag{17}$$

where the thermal properties have been compacted into the definition of the thermal diffusivity

$$\alpha \equiv \frac{k}{\rho c_p}$$

This equation is now integrated for the second time and the second boundary condition is applied indirectly. Instead of using Eq. (10) immediately, it is more convenient to introduce now the centreline temperature T_c and to relate it at a later stage with the wall heat flux, by making use of the definitions for $\dot{q}_w$ and the bulk temperature $\bar{T}$. Thus, the temperature distribution becomes

$$T - T_c = \frac{2\overline{u_N}R^2}{\alpha}\frac{\mathrm{d}T}{\mathrm{d}x}\left[\frac{1+a}{4}\left(\frac{r}{R}\right)^2-\frac{1}{16}\left(\frac{r}{R}\right)^4-\frac{a}{36}\left(\frac{r}{R}\right)^6\right] - \frac{16\eta\overline{u_N}^2}{k}\left[\frac{1}{16}\left(\frac{r}{R}\right)^4+\frac{a}{18}\left(\frac{r}{R}\right)^6\right] \tag{18}$$

The wall temperature is easily obtained from Eq. (18) by setting $T = T_w$ at $r/R = 1$ and is given by

$$T_w - T_c = \frac{\overline{u_N}R^2}{2\alpha}\frac{\mathrm{d}T}{\mathrm{d}x}\left[\frac{3}{4}+\frac{8}{9}a\right] - \frac{\eta\overline{u_N}^2}{k}\left[1+\frac{8}{9}a\right] \tag{19}$$

Note that in Eqs. (17)–(19) the second term on the right-hand-side comes from the inclusion of the viscous dissipation function in the energy equation, and the elastic/extensional capacity of the fluid is buried in parameter a, as defined at the end of the previous section (Eq. (16b)).

The wall heat flux $\dot{q}_w$ allows the definition of the heat transfer coefficient (h) for this forced convection flow as

$$\dot{q}_w \equiv h(\bar{T} - T_w) \tag{20}$$

where the cross-section average temperature is defined as

$$\bar{T} \equiv \frac{\int_0^R 2\pi u T r \, dr}{\int_0^R 2\pi u r \, dr} \tag{21}$$

The denominator of Eq. (21) represents the volumetric flow rate $\pi R^2 \bar{u}$. Oliveira and Pinho [9] derived analytically a useful expression for the bulk velocity

$$\bar{u} = \overline{u_N}\left(1 + \frac{4}{3}a\right) \tag{22}$$

to be used in the ensuing analysis. Note, however, that a still depends on $\bar{u}$. Upon substitution, integration of Eq. (21) yields the bulk temperature

$$\bar{T} - T_c = \frac{\frac{\overline{u_N} R^2}{\alpha}\frac{dT}{dx}\left[\frac{13}{54}a^2 + \frac{17}{45}a + \frac{7}{48}\right] - \frac{\eta \overline{u_N}^2}{3k}\left[\frac{4}{9}a^2 + \frac{16}{15}a + \frac{1}{2}\right]}{1 + \frac{4}{3}a} \tag{23}$$

The boundary condition (10) is now introduced through the heat transfer coefficient

$$h = \frac{-k\left(\frac{\partial T}{\partial r}\right)_{r=R}}{\bar{T} - T_w} \tag{24a}$$

which is calculated next and presented in nondimensional form as a Nusselt number

$$Nu \equiv \frac{D_H h}{k} = \frac{2Rh}{k} \tag{24b}$$

After performing the necessary substitutions in Eqs. (24a) and (24b) we obtain:

$$Nu = \frac{\left[\frac{\overline{u_N} R^2}{\alpha}\frac{dT}{dx} - \frac{8\eta \overline{u_N}^2}{k}\right]\left[1 + \frac{4}{3}a\right]^2}{\frac{\overline{u_N} R^2}{\alpha}\frac{dT}{dx}\left[\frac{19}{54}a^2 + \frac{17}{30}a + \frac{11}{48}\right] - \frac{\eta \overline{u_N}^2}{k}\left[\frac{28}{27}a^2 + \frac{28}{15}a + \frac{5}{6}\right]} \tag{25}$$

Eq. (25) is still not in a convenient format because it depends on some dimensional quantities. In the absence of viscous dissipation, equivalent to setting $\eta = 0$, Eq. (25) would depend exclusively on a, which is a dimensionless measure of elasticity.

The viscous dissipation is conveniently accounted for by the dimensionless Brinkman number and in this work we use the modified version defined by Shah and London [13] for a prescribed heat flux:

$$Br \equiv \frac{\eta \bar{u}^2}{D_H \dot{q}_w} = \frac{\eta \bar{u}^2}{2R\dot{q}_w} \tag{26}$$

where D_H is the hydraulic diameter, here equal to $2R$. Using Eq. (22) we get a relationship between Br and $\eta \overline{u_N}^2$

$$\eta \overline{u_N}^2 = \frac{2R\dot{q}_w Br}{\left[1 + \frac{4}{3}a\right]^2} \tag{27}$$

Since $\dot{q}_w = -k\partial T/\partial r|_{r=R} = [\frac{4\eta \overline{u_N}^2}{R} - (k\overline{u_N}R/2\alpha)\, dT/dx][1 + 4/3a]$, and using Eq. (27), we relate the modified Brinkman number to the longitudinal temperature gradient

$$\frac{\overline{u_N} R}{\alpha}\frac{dT}{dx} = \frac{2\dot{q}_w}{k}\frac{\left[8Br - 1 - \frac{4}{3}a\right]}{\left[1 + \frac{4}{3}a\right]^2} \tag{28}$$

Finally, we can use Eqs. (27) and (28) to obtain a more useful expression for the Nusselt number

$$Nu = \frac{\left[1 + \frac{4}{3}a\right]^2}{\left[\frac{19}{54}a^2 + \frac{17}{30}a + \frac{11}{48}\right] - Br\left[1 + \frac{4}{3}a\right]} \tag{29}$$

Eq. (29) reduces to well-known Newtonian solutions: for no elasticity ($a = 0$) and negligible viscous dissipation ($Br = 0$) it reduces to $Nu = 4.364$ (Holman [14]), but for nonnegligible dissipation Eq. (29) becomes

$$Nu = \frac{48}{11 - 48Br} \tag{30}$$

an expression in agreement with the Newtonian fluid derivation.

The above equation for the temperature profile $T(r)$ can also be cast into a nondimensional form using the usual definition

$$\theta(r) \equiv \frac{T(r) - T_w}{\overline{T} - T_w} \tag{31}$$

which, together with the use of the modified Brinkman number, is given by

However, as will be shown in Section 4, the dimensionless temperature defined by Eq. (31) is not convenient when viscous dissipation is present and improved understanding of the phenomena involved will require a different scaling. This will make use of the following expressions:

$$\theta(r) = \frac{2\left[8Br - 1 - \frac{4}{3}a\right]\left[1 + \frac{4}{3}a\right]\left\{\frac{1+a}{4}\left(\frac{r}{R}\right)^2 - \frac{1}{16}\left(\frac{r}{R}\right)^4 - \frac{a}{36}\left(\frac{r}{R}\right)^6 - \frac{3}{16} - \frac{8}{36}a\right\}}{Br\left[\frac{28}{27}a^2 + \frac{28}{15}a + \frac{5}{6}\right] + \left[1 + \frac{4}{3}a - 8Br\right]\left[\frac{19}{54}a^2 + \frac{17}{30}a + \frac{11}{48}\right]}$$
$$- \frac{Br\left[1 + \frac{4}{3}a\right]\left\{\left(\frac{r}{R}\right)^4 + \frac{8}{9}a\left(\frac{r}{R}\right)^6 - 1 - \frac{8}{9}a\right\}}{Br\left[\frac{28}{27}a^2 + \frac{28}{15}a + \frac{5}{6}\right] + \left[1 + \frac{4}{3}a - 8Br\right]\left[\frac{19}{54}a^2 + \frac{17}{30}a + \frac{11}{48}\right]} \tag{32}$$

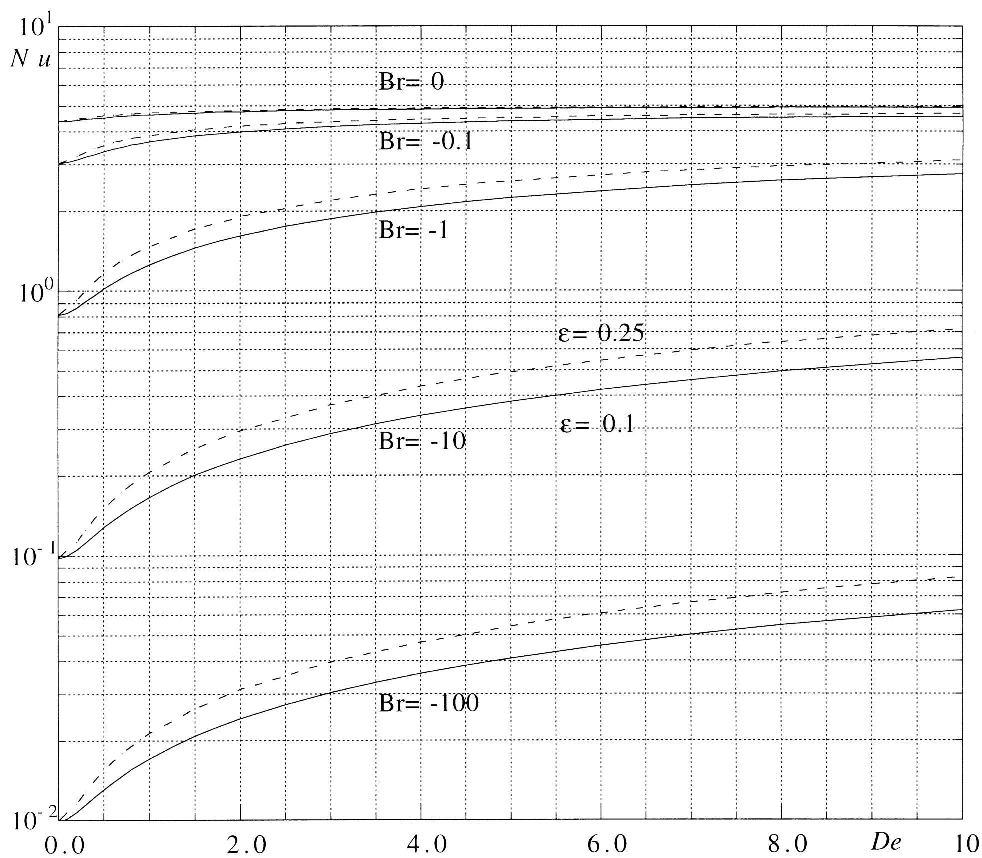

Fig. 1. Variation of the Nusselt number as a function of the Deborah number, Brinkman number and ε, in the case of wall heating. Due to $\dot{q}_w$ convention, Br is negative for wall heating.

$$\frac{(T_w - T_c)k}{\dot{q}_w R} = \frac{4Br - \frac{3}{4} - \frac{8}{9}a}{1 + \frac{4}{3}a} \tag{33}$$

$$\frac{(\overline{T} - T_c)k}{\dot{q}_w R} = \frac{2Br}{1 + \frac{4}{3}a} - \frac{2\left[\frac{13}{54}a^2 + \frac{17}{45}a + \frac{7}{48}\right]}{\left[1 + \frac{4}{3}a\right]^2} \tag{34}$$

$$\frac{(\overline{T} - T_w)k}{\dot{q}_w R} = \frac{\frac{19}{27}a^2 + \frac{17}{15}a + \frac{11}{24}}{\left[1 + \frac{4}{3}a\right]^2} - \frac{2Br}{1 + \frac{4}{3}a} \tag{35}$$

3.2. Channel flow

For the channel flow the analytical derivation is similar and is based on the hydrodynamic solution of Oliveira and Pinho [9]. The analysis starts with the set of equations corresponding to Eqs. (7)–(15), (16a) and (16b) for the plane channel and the results of such effort are presented now without any other details. The transverse coordinate is y and the channel half-width is equal to H.

For this flow geometry we use

$$a \equiv 9\varepsilon De^2 \left(\frac{\overline{u_N}}{\bar{u}}\right)^2 \tag{36}$$

and we obtain the following results. The transverse distribution of temperature is

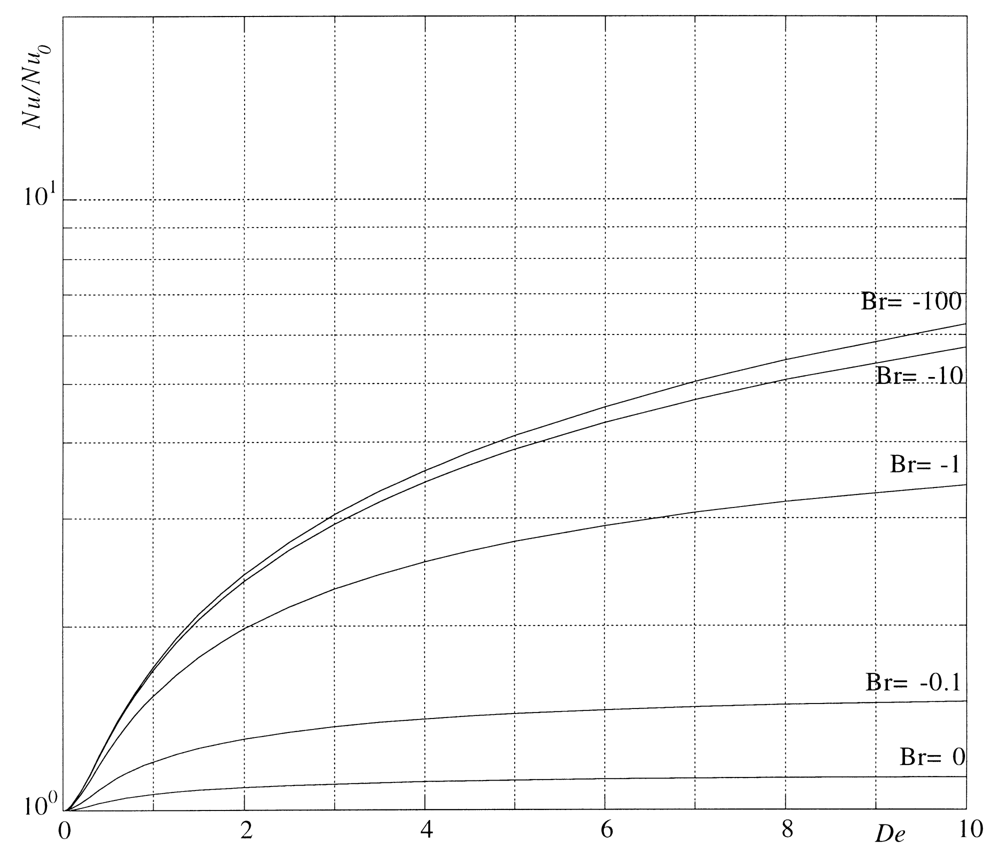

Fig. 2. Relative variation of the Nusselt number as a function of the Deborah number and Brinkman number for wall heating and $\varepsilon = 0.1$. Due to $\dot{q}_w$ convention, Br is negative for wall heating.

$$T - T_c = \frac{3\overline{u_N}H^2}{2\alpha}\frac{dT}{dx} \times \left[\frac{1+a}{2}\left(\frac{y}{H}\right)^2 - \frac{1}{12}\left(\frac{y}{H}\right)^4 - \frac{a}{30}\left(\frac{y}{H}\right)^6\right] - \frac{9\eta\overline{u_N}^2}{k}\left[\frac{1}{12}\left(\frac{y}{H}\right)^4 + \frac{a}{15}\left(\frac{y}{H}\right)^6\right] \tag{37a}$$

and in nondimensional form

$$\theta(y) = \frac{\left[12Br - 1 - \frac{6}{5}a\right]\left[1 + \frac{6}{5}a\right]\left\{\frac{1+a}{2}\left(\frac{y}{H}\right)^2 - \frac{1}{12}\left(\frac{y}{H}\right)^4 - \frac{a}{30}\left(\frac{y}{H}\right)^6 - \frac{5}{12} - \frac{7}{15}a\right\}}{24Br\left[\frac{144}{1925}a^2 + \frac{16}{105}a + \frac{8}{105}\right] + \left[1 + \frac{6}{5}a - 12Br\right]\left[\frac{808}{1925}a^2 + \frac{232}{315}a + \frac{102}{315}\right]} - \frac{24Br\left[1 + \frac{6}{5}a\right]\left\{\frac{1}{12}\left(\frac{y}{H}\right)^4 + \frac{a}{15}\left(\frac{y}{H}\right)^6 - \frac{1}{12} - \frac{a}{15}\right\}}{24Br\left[\frac{144}{1925}a^2 + \frac{16}{105}a + \frac{8}{105}\right] + \left[1 + \frac{6}{5}a - 12Br\right]\left[\frac{808}{1925}a^2 + \frac{232}{315}a + \frac{102}{315}\right]} \tag{37b}$$

From Eq. (37a) we get the wall temperature by setting $y/H = 1$

$$T_w - T_c = \frac{3\overline{u_N}H^2}{4\alpha}\frac{dT}{dx}\left[\frac{5}{6} + \frac{14}{15}a\right] - \frac{9\eta\overline{u_N}^2}{k}\left[\frac{1}{12} + \frac{a}{15}\right] \tag{38}$$

The cross-sectional average temperature is given by

$$\bar{T} - T_c = \frac{\frac{9\overline{u_N}H^2}{20\alpha}\frac{dT}{dx}\left[\frac{108}{231}a^2 + \frac{145}{189}a + \frac{13}{42}\right] - \frac{27\eta\overline{u_N}^2}{2k}\left[\frac{12}{3465}a^2 + \frac{1}{105}a + \frac{1}{210}\right]}{1 + \frac{6}{5}a} \tag{39}$$

The final expression for the Nusselt number ($Nu \equiv \frac{4Hh}{k}$) becomes

$$Nu = \frac{4\left[1 + \frac{6}{5}a\right]^3}{\left[1 + \frac{6}{5}a - 12Br\right]\left[\frac{1212}{1925}a^2 + \frac{116}{105}a + \frac{17}{35}\right] + 4Br\left[\frac{1296}{1925}a^2 + \frac{48}{35}a + \frac{24}{35}\right]} \tag{40}$$

Similarly to the pipe flow, Eq. (40) reduces to the well known Newtonian value of $Nu = 8.235$ when $a = 0$ and $Br = 0$, and to

$$Nu = \frac{140}{17 - 108Br} \tag{41}$$

for the Newtonian flow case with viscous dissipation. The viscous dissipation contribution to the temperature profile for a Newtonian fluid is in agreement with the results in Schlichting [15].

4. Discussion of results

In the absence of viscous dissipation the solution is independent of whether there is wall cooling or heating. However, viscous dissipation always contributes to internal heating of the fluid, hence the solution will differ according to the process taking place at the wall.

4.1. Negative heat flux at the wall (wall heating)

According to the definition of wall heat flux adopted here (see Eq. (10)) a negative value of $\dot{q}_w$ implies that heat is being supplied across the walls into the fluid and Eq. (26) requires that $Br < 0$. In this case Eq. (28) implies a positive longitudinal gradient of temperature ($dT/dx > 0$), i.e. the fluid is always being heated. Fig.

1 shows the variation of the Nusselt number with the Deborah number, the modified Brinkman number and the extensional parameter ε of the constitutive equation. There is a strong influence of viscous dissipation on the heat transfer coefficient which is also affected by fluid elasticity (De) and the extensional capabilities ($\varepsilon \neq 0$) of the fluid. For an elastic fluid devoid of extensional characteristics ($\varepsilon = 0$), Nu remains equal to the corresponding value at $De = 0$, even for $De > 0$. In the absence of viscous dissipation effects the Nusselt number increases from the Newtonian value of 4.364 to the asymptotic value of 5.053 which is independent of the value of ε and De. As the magnitude of the modified Brinkman number increases the Nusselt number decreases and simultaneously the role of elasticity is enhanced: the relative variation of the Nusselt number with the Deborah number becomes more pronounced, as can be observed in Fig. 2. In this figure, the ratio of Nu to the corresponding value Nu_0 for $De = 0$ is shown as a function of De for different values of Br. A threefold increase of Nusselt number is seen to occur for Brinkman numbers as low as -1.

The decrease in Nusselt number with viscous dissipation is a consequence of the increased temperature range within the pipe and namely of the difference $T_w - \bar{T}$ for a constant heat flux. Based on the same argument, an increase in Nusselt number by elasticity is synonymous to the reduction in temperature differences within the pipe. This reduction of the temperature differences stems from an improved heat transfer in the wall region due to the higher velocity gradients there, at high values of the Deborah number (check Fig. 2 of Oliveira and Pinho [9]).

The effect of ε is similar to that of the Deborah number as can be confirmed in the radial profiles of the normalised temperatures in Fig. 3 which compare $\varepsilon = 0.1$ and $\varepsilon = 0.25$. This is to be expected since elasticity is quantified by the function a containing both ε and De contributions. It is not apparent from Eqs. (16a) and (16b) how a will

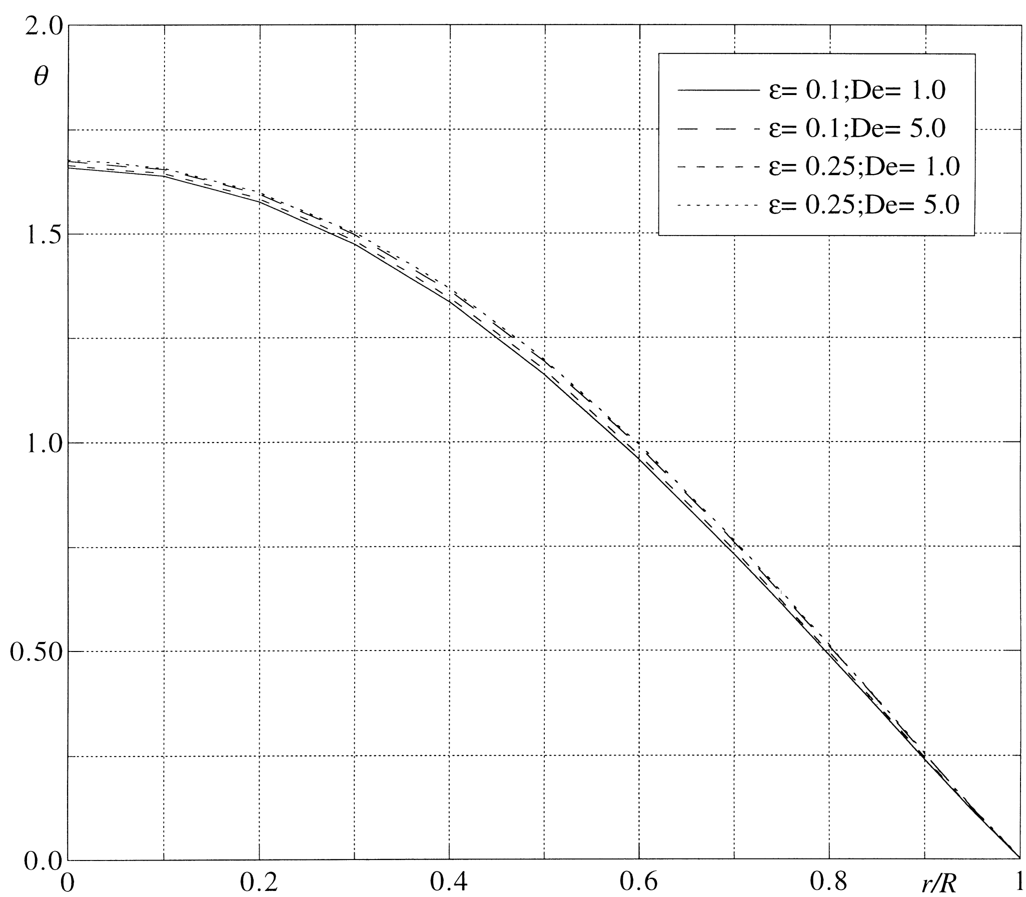

Fig. 3. Effect of ε on the radial variation of the standard normalised temperature θ for negligible viscous dissipation ($Br = 0$).

vary when ε and De are increased but the results in Oliveira and Pinho [9] show that a does increase indeed with $\sqrt{\varepsilon}De$. One should also keep in mind that an increase in ε is actually related to a reduction of the extensional viscosity of the fluid and not with shear elasticity, this is measured by the shear relaxation time of the fluid. In this respect, the present results are very important because they show that an elastic fluid with extensional characteristics (measured by ε) have heat transfer characteristics, in fully developed duct flow, substantially different from an elastic fluid without extensibility. Indeed, if we take a fluid obeying the upper convected Maxwell equation, which has no capacity for extension ($\varepsilon = 0$) but is clearly elastic, we see that its heat transfer characteristics are coincident with those for a Newtonian fluid.

The standard way of making temperature nondimensional, based on Eq. (31) and exemplified in Fig. 3, is not appropriate for the situation of imposed heat-flux because the temperature scale $\Delta T = \bar{T} - T_w$ varies with the relevant parameters and may lead to misinterpretation of the corresponding variation of T. For example, in Fig. 3 the gradient of this standard dimensionless temperature is seen to vary with elasticity near the wall, while the actual temperature gradient is constant for the given $\dot{q}_w$. In fact, for a given $\dot{q}_w$, the unknown of the problem is ΔT and it is thus more convenient to define a fixed temperature scale that we take as $\dot{q}_w R/k$. Fig. 4 shows two sets of temperature profiles made nondimensional with this fixed scale, for $Br = -1$ and $Br = -10$, and various Deborah numbers (at $\varepsilon = 0.1$). This plot makes clear the aforementioned effects of increased elasticity and reduced dissipation in reducing the range of temperature variation across the pipe section and consequently leading to higher Nusselt numbers.

Note also that with this normalisation of the temperature the slope of the curves near the wall must be equal to -1 for all cases, as is apparent in Fig. 4.

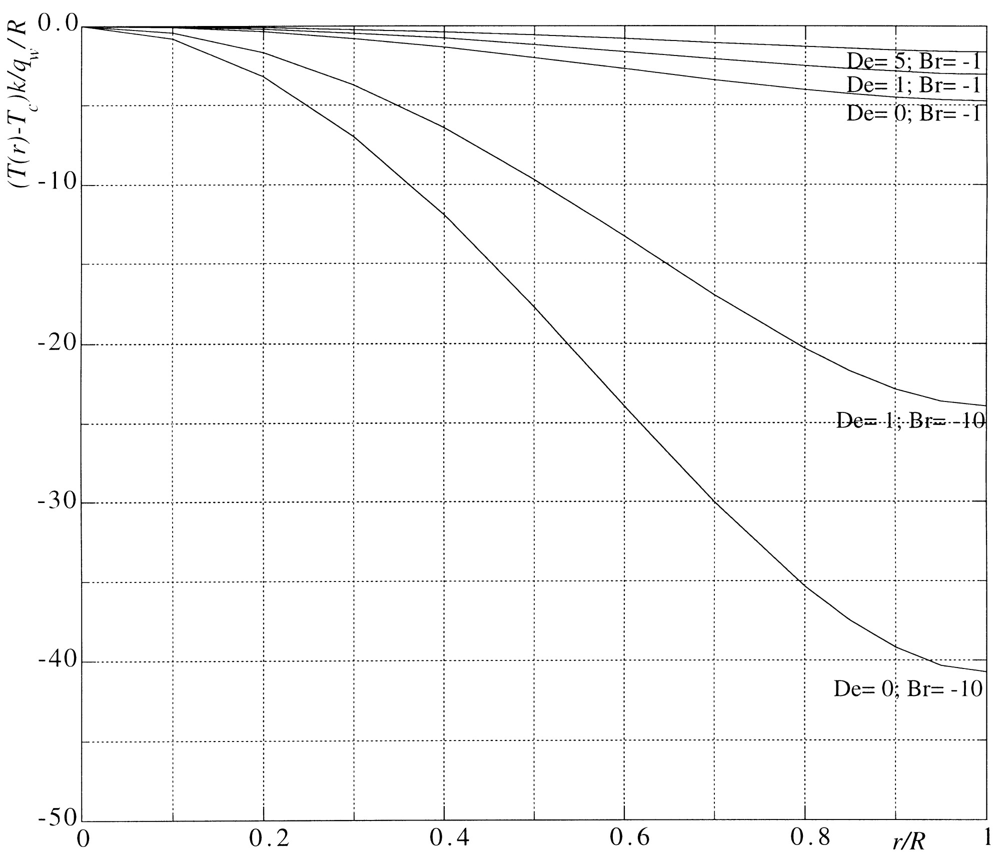

Fig. 4. Radial profiles of the normalised temperature for wall heating ($Br = -1$ and $Br = -10$), as a function of Deborah number and for $\varepsilon = 0.1$.

4.2. Positive heat flux at the wall (wall cooling)

Wall cooling ($\dot{q}_w > 0$) is applied to reduce the bulk temperature of the fluid but, as for the Newtonian case, the amount of viscous dissipation may change the overall heat balance: for low positive values of Br, a positive wall heat flux leads to a consistent decrease in temperature, $dT/dx < 0$ (cf. Eq. (28)); however, if Br exceeds a certain limiting value, the heat generated internally by viscous processes will overcome the effect of wall cooling. This limiting condition is obtained after equating to zero the gradient of temperature in Eq. (28), to give

$$Br_1 = \frac{1}{8} + \frac{a}{6} \tag{42}$$

Above this critical Brinkman number the fluid heats up ($dT/dx > 0$) and the Nusselt number, as defined by Eqs. (24a) and (24b), is positive. This Nusselt number must be interpreted cautiously because there exists a second critical Brinkman number defined by

$$Br_2 = \frac{\frac{19}{54}a^2 + \frac{17}{30}a + \frac{11}{48}}{1 + \frac{4}{3}a} \tag{43}$$

At $Br = Br_2$, Eq. (35) shows that $\bar{T} = T_w$ leading to an undefined Nu (in fact infinite since $Nu = 2R\dot{q}_w/(k(\bar{T} - T_w))$). The Br value of Eq. (43) thus gives a mathematical singularity for the definition of Nusselt number here adopted. Above the second critical value of Br the Nusselt number switches to negative, expressing in this way the relative change in the magnitude of both temperatures, not a change in the direction of the wall heat flux.

The radial temperature profiles change according to the range of Brinkman number and Fig. 5 shows typical profiles in each of the zones of positive Brinkman number behaviour, including the case of negligible viscous dissipation. Note that for the specific case of Fig. 5, the critical Brinkman numbers are $Br_1 = 0.516$ and

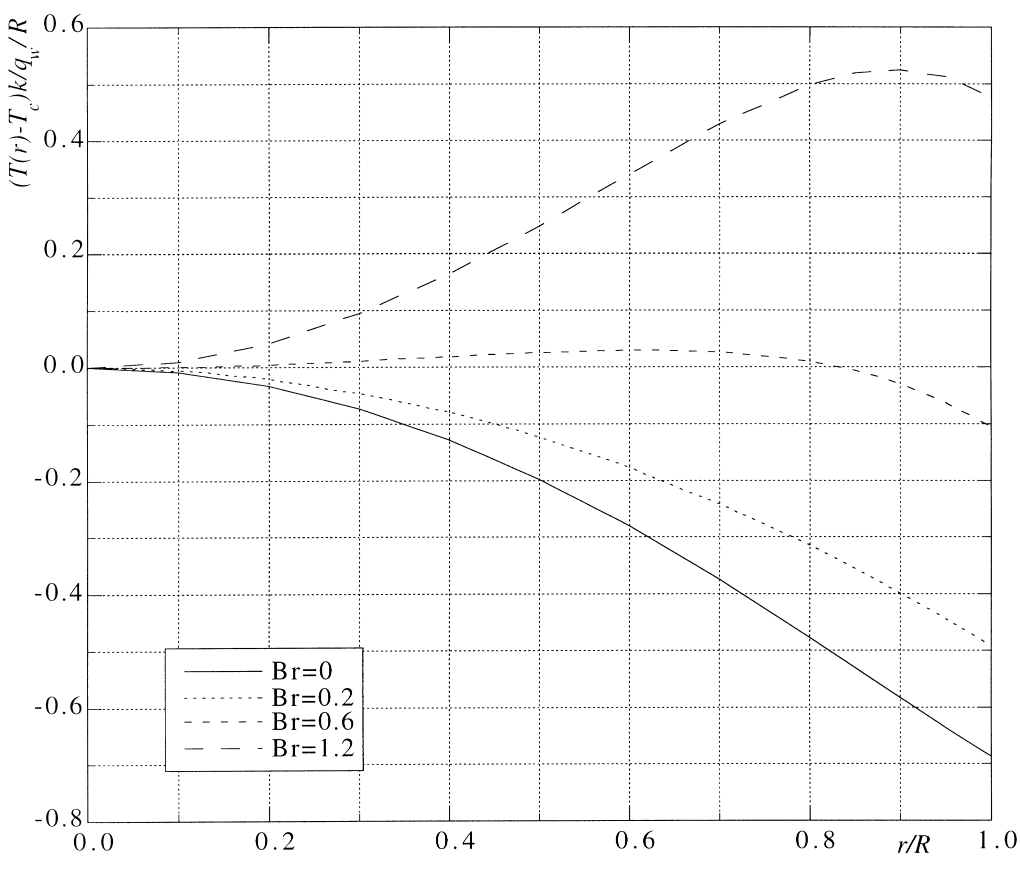

Fig. 5. Radial profile of the normalised temperature as a function of the Brinkam number for $De = 5$ and $\varepsilon = 0.1$.

$Br_2 = 0.847$. Thus, the curves for $Br = 0.6$ and 1.2 already exhibit the effect of fluid heating up due to dissipation ($\bar{T} > T_c$) although the slope at the wall must remain equal to -1. These behaviours are analogous to those of Newtonian fluids for cooled wall boundary layer, and the novelty here is that the boundaries between the various regions change with elasticity. This effect, and that of the material parameter ε will be analysed next.

Fig. 6 shows the variation of $(T_w - T_c)/k\dot{q}_w R$ from Eq. (33) and $(\bar{T} - \bar{T}_c)/k\dot{q}_w R$ from Eq. (34) as a function of the modified Brinkman number, for a Newtonian fluid ($De = 0$) and an elastic fluid ($De = 5$) with two values of the extensional parameter ($\varepsilon = 0.1$ and 0.25). Those temperatures follow a straight line variation and, for each De and ε, say $De = 0$, the two lines cross at the second critical Brinkman number (Eq. (43)). Higher values of the Deborah number and of ε always reduce the slope of the curves, with the former parameter having a stronger influence than the latter. Simultaneously, the value of the second critical Brinkman number Br_2 increases and the dashed straight lines in Fig. 6 cross at $Br_2 = 0.847$ for $\varepsilon = 0.1$ and at $Br_2 = 1.111$ for $\varepsilon = 0.25$ (this second value is further to the right of the x-axis limit). This effect of elasticity on the critical Brinkman numbers is clarified in Fig. 7 where Br_1 and Br_2 are shown as a function of De, for three values of the extensional parameter: $\varepsilon = 0.01$ (small extensional capacity), $\varepsilon = 0.1$ and $\varepsilon = 0.25$ (larger extensional capacity, typical of polymer melts).

The variation of both critical Brinkman numbers with the Deborah number and the parameter ε is similar: both increase in a similar way, with Br_2 always higher than Br_1. The role of fluid elasticity is thus that of extending the range of Brinkman numbers over which there is cooling of the fluid, when heat is extracted at the wall, which is equivalent to saying that there is a reduction of the effects of viscous dissipation. This is consistent with the strong reduction in temperature differences observed with elastic fluids (compare curves for T_w and $\bar{T}$ in Fig. 6 at identical conditions). Since elasticity reduces temperature differences, the

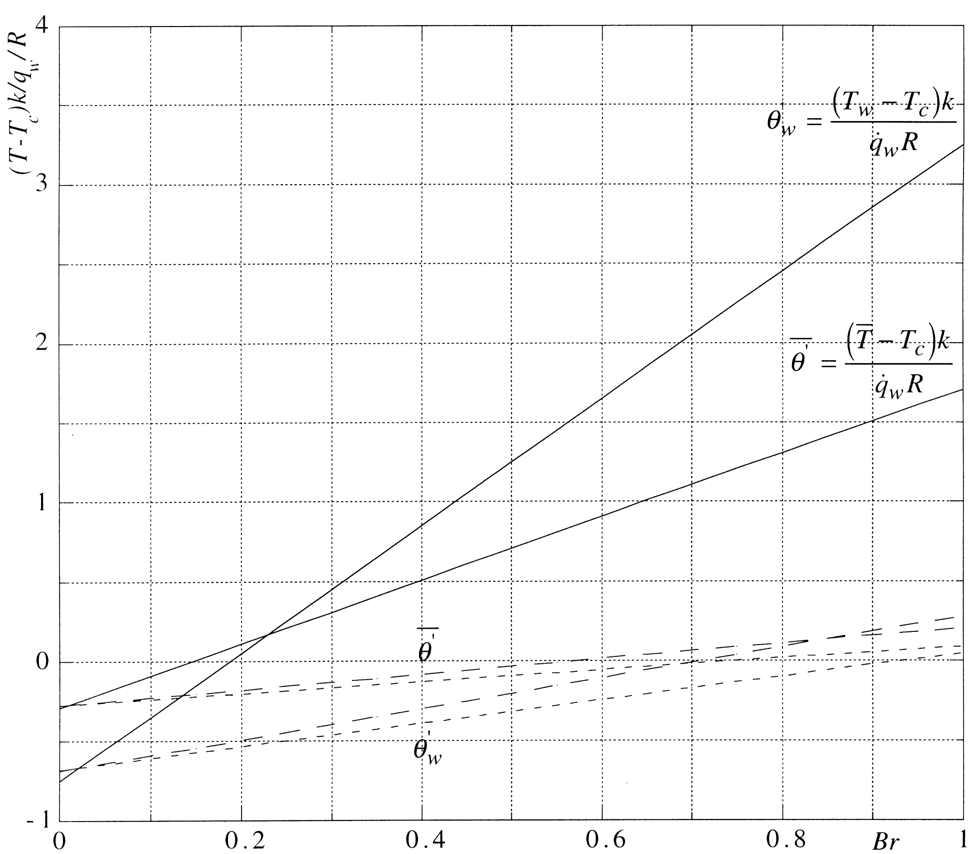

Fig. 6. Variation of the normalised bulk and wall temperatures with the Brinkman number for the cases without ($De = 0$, solid) and with ($De = 5$, dashed) elasticity. Two values of ε are considered: 0.1 (long-dash) and 0.25 (short-dash).

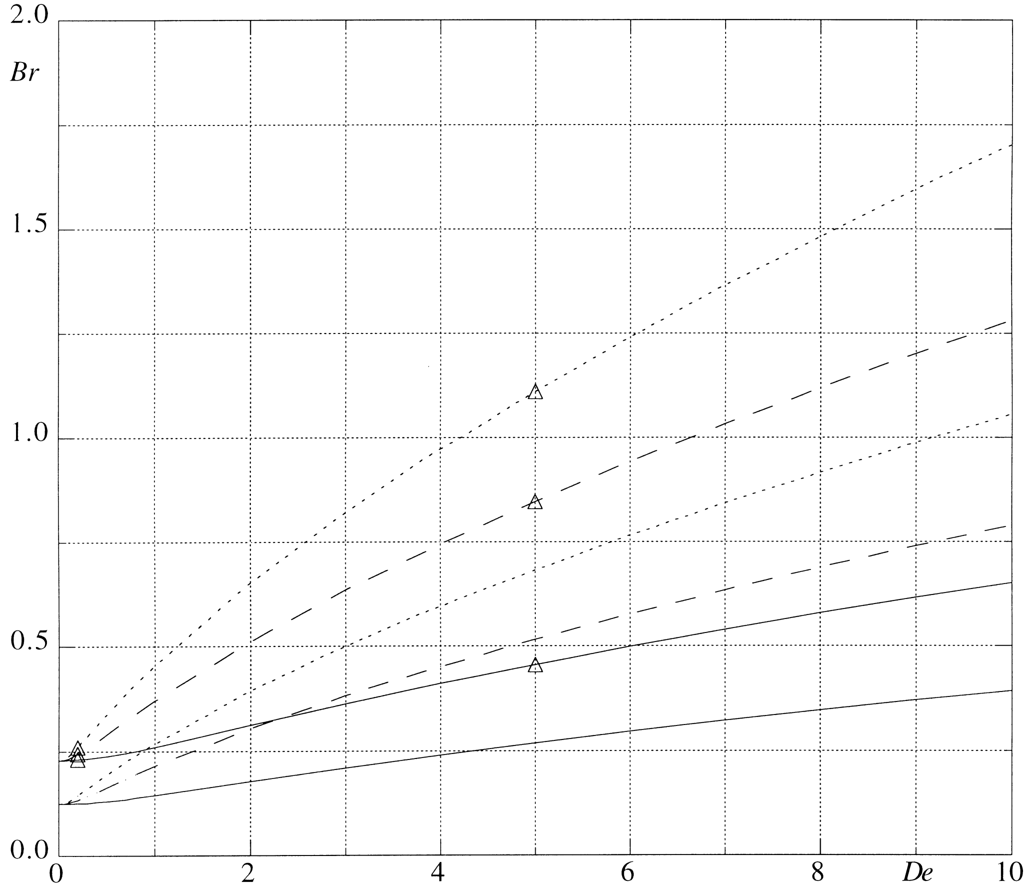

Fig. 7. Variation of the two critical Brinkman numbers with the Deborah number and the material parameter ε: Br_1: (no symbol); Br_2:(Δ). $\varepsilon = 0.01$ (full line); $\varepsilon = 0.1$ (long dashes); $\varepsilon = 0.25$ (short dashes).

fluid can sustain higher intensities of viscous dissipation before the reversal of overall fluid 'heating/cooling' behaviour. The plug-like velocity profile and higher shear rates in the wall region of more viscoelastic fluids simultaneously increase the amount of fluid flowing near the wall and the heat transfer coefficient, as a consequence of the shorter radial distance the heat flux must traverse to heat the fluid.

Finally, in Fig. 8 the Nusselt number for $Br > Br_2$ is plotted as a function of the Deborah number. The increase of viscous dissipation for $Br > Br_2$ leads to increased temperature differences and consequently to a reduction of the Nusselt number in absolute terms.

For the channel flow similar conclusions can be drawn from a similar study.

4.3. Empirical correlation for engineering

The use of Eq. (29) for engineering purposes, as in polymer processing extrusion, is complicated by the need to calculate the ratio $\overline{u_N}/\bar{u}$ in Eq. (16). Both that ratio and function a depend on ε and De and a simpler alternative to calculate the Nusselt number relies on the following correlation for a

$$a = 0.0513\sqrt{\varepsilon}De - 1.68\left(\sqrt{\varepsilon}De\right)^{0.329} + 3.235\left(\sqrt{\varepsilon}De\right)^{0.58} \tag{44}$$

and the use of Eq. (29)

$$Nu = \frac{\left[1 + \frac{4}{3}a\right]^2}{\left[\frac{19}{54}a^2 + \frac{17}{30}a + \frac{11}{48}\right] - Br\left[1 + \frac{4}{3}a\right]}$$

With Eq. (44) only the fluid parameters (ε and λ) and the bulk velocity ($\bar{u}$) are required and the Nusselt number calculated in this way is well within 1% of that given by the exact solution for values of $\sqrt{\varepsilon}De$ between 0.1 and 300. For lower values of $\sqrt{\varepsilon}De$ the Nusselt

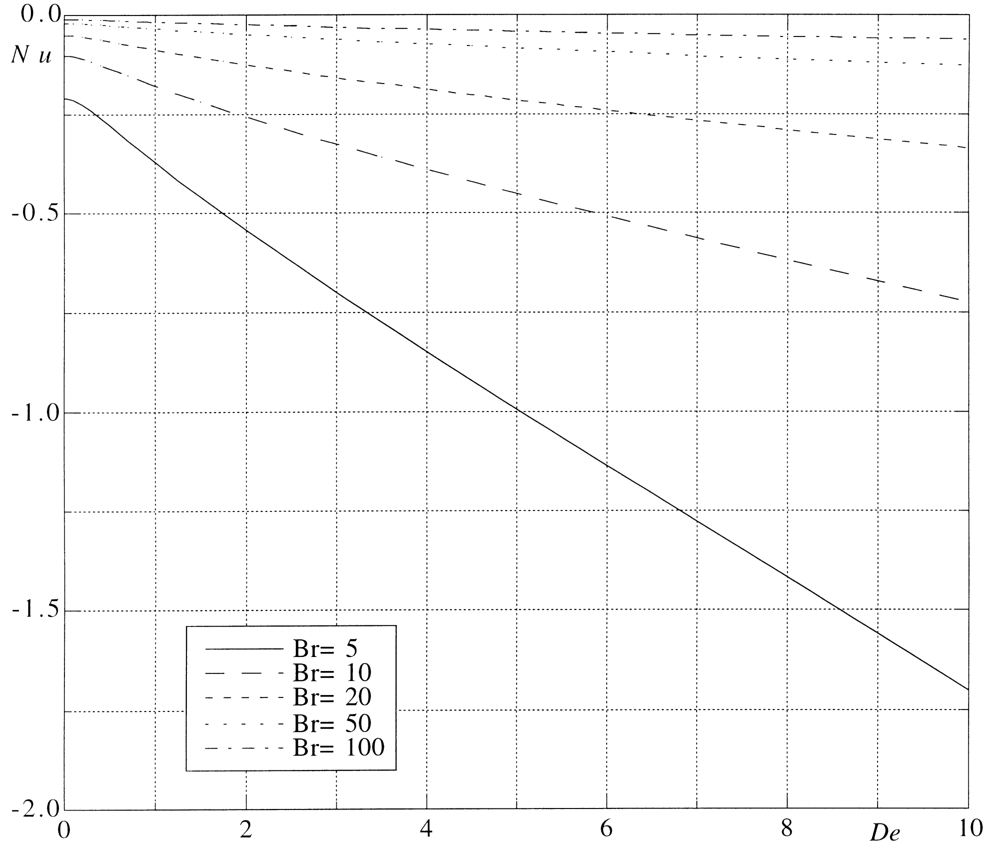

Fig. 8. Variation of the Nusselt number with the Deborah and Brinkman numbers for wall cooling, $\varepsilon = 0.1$ and $Br > Br_2$.

number is close to that of the corresponding Newtonian case.

5. Conclusions

Temperature distributions and heat transfer coefficients were obtained in pipe and channel flows of a simplified Phan-Thien–Tanner fluid when the stress coefficient assumed a linear form and the effect of temperature variations on the material parameters was neglected. The analytical solution includes the effect of viscous dissipation.

In all circumstances, i.e. for wall heating and cooling and regardless of the magnitude of viscous dissipation, an increase of fluid elasticity (De) and/or an increase of ε results in enhanced heat transfer provided $\varepsilon \neq 0$. It was found that these effects of fluid elasticity (De) and extensibility (ε), as measured by the parameter a and indirectly by $\sqrt{\varepsilon}De$, are greatly enhanced by viscous dissipation, here quantified by a modified Brinkman number. For example, for vanishing viscous dissipation there is an increase of 9% in the Nusselt number when De rises from 0 to 2 (at $\varepsilon = 0.1$), but this increase in Nu attains a value of 31% when the level of dissipation is just $Br = -0.1$

For wall cooling and whenever the Brinkman number exceeds a critical value (Br_1 in Eq. (42)), the heat generated by viscous dissipation overcomes the heat removed at the wall and the fluid heats up longitudinally. Fluid elasticity and extensibility delays this critical Brinkman number to higher values.

Purely elastic fluids ($\varepsilon = 0$) have heat transfer characteristics equal to those of Newtonian fluids.

Acknowledgements

P.J. Oliveira would like to thank the financial support of Fundação para a Ciência e Tecnologia through the sabbatical grant FMRH/BSAB/68/99.

References

[1] N. Phan-Thien, R.I. Tanner, A new constitutive equation derived from network theory, J. Non-Newt. Fluid Mech 2 (1977) 353–365.

[2] L.M. Quinzani, R.C. Armstrong, R.A. Brown, Use of coupled birefringence and LDV studies of flow through a planar contraction to test constitutive equations for concentrated polymer solutions, J. Rheology 39 (1995) 1201–1228.

[3] H.M. Laun, H. Schuch, Transient elongational viscosities and drawability of polymer melts, J. Rheol 33 (1989) 119–175.

[4] G.H. Wu, S.J. Ju, C.C. Wu, Numerical prediction of non-isothermal flow of nylon-6 past a cylinder between plates, J. Polymer Eng 19 (1999) 27–38.

[5] N. Phan-Thien, A nonlinear network viscoelastic model, J. Rheol 22 (1978) 259–283.

[6] R.G. Larson, Constitutive Equations for Polymer Melts and Solutions, Butterworths, Boston, 1988.

[7] R.I. Tanner, Engineering Rheology, Clarendon Press, Oxford, 1985.

[8] G.W.M. Peters, J.F.M. Schoonen, F.P.T. Baaijens, H.E.H. Meijer, On the performance of enhanced constitutive models for polymer melts in a cross-slot flow, J. Non-Newt. Fluid Mech 82 (1999) 387–427.

[9] P.J. Oliveira, F.T. Pinho, Analytical solution for fully-developed channel and pipe flow of Phan-Thien–Tanner fluids, J. Fluid Mech 387 (1999) 271–280.

[10] T.F. Irvine, Jr., J. Karni, Non-Newtonian fluid flow and heat transfer, in: S. Kakaç, R.K. Shah, W. Aung (Eds.), Handbook of Single-Phase Convective Heat Transfer, Wiley, New York, pp. 20.1–20.57.

[11] Z. Tadmor, C.G. Gogos, Principles of Polymer Processing, 1st ed., Wiley, New York, 1979.

[12] R.B. Bird, R.C. Armstrong, O. Hassager, Dynamics of Polymeric Liquids. Volume 1: Fluid Dynamics, 2nd ed., John Wiley, New York, 1987.

[13] R.K. Shah, A.L. London, Laminar Flow Forced Convection in Ducts, Academic Press, New York, 1978.

[14] J.P. Holman, Heat Transfer, 5th ed., McGraw-Hill, New York, 1981.

[15] H. Schlichting, Boundary-layer Theory, 6th ed., McGraw-Hill, New York, 1968.